



**HAL**  
open science

# Polydopamine-based molecularly imprinted thin films for electro-chemical sensing of nitro-explosives in aqueous solutions

Nadja Leibl, Luminita Duma, Carlo Gonzato, Karsten Haupt

## ► To cite this version:

Nadja Leibl, Luminita Duma, Carlo Gonzato, Karsten Haupt. Polydopamine-based molecularly imprinted thin films for electro-chemical sensing of nitro-explosives in aqueous solutions. *Bioelectrochemistry*, 2020, 135, pp.107541. 10.1016/j.bioelechem.2020.107541 . hal-02881036

**HAL Id: hal-02881036**

**<https://hal.science/hal-02881036>**

Submitted on 25 Jun 2020

**HAL** is a multi-disciplinary open access archive for the deposit and dissemination of scientific research documents, whether they are published or not. The documents may come from teaching and research institutions in France or abroad, or from public or private research centers.

L'archive ouverte pluridisciplinaire **HAL**, est destinée au dépôt et à la diffusion de documents scientifiques de niveau recherche, publiés ou non, émanant des établissements d'enseignement et de recherche français ou étrangers, des laboratoires publics ou privés.

# Polydopamine-based molecularly imprinted thin films for electrochemical sensing of nitro-explosives in aqueous solutions

Nadja Leibl,<sup>†, ‡</sup> Luminita Duma,<sup>†</sup> Carlo Gonzato<sup>†</sup> and Karsten Haupt<sup>†</sup>

<sup>†</sup>Sorbonne Universités, Université de Technologie de Compiègne, Enzyme and Cell Engineering Laboratory, UMR CNRS 7025, Rue Roger Couitolenc, CS 60319, 60203 Compiègne Cedex, France

<sup>‡</sup>Present address: Université du Sud Toulon, Laboratoire Matériaux Polymères-Interfaces-Environnement Marin, 83957 La Garde Cedex, France

**KEYWORDS** Nitro-explosives, 2,4,6-trinitrotoluene, RDX, polydopamine, thin films, chemosensor, electropolymerization, molecularly imprinted polymers, cyclic voltammetry.

---

**ABSTRACT:** A sensitive electrochemical sensor was developed for the detection of nitro-explosives in aqueous solutions based on thin molecularly imprinted polydopamine films. Dopamine was identified *in silico*, based on DFT (density functional theory) calculations with the  $\omega$ B97X-D/6-31G\* basis set, as the best functional monomer and electropolymerized via cyclic voltammetry (CV) in the presence of carboxylic acid-based structural analogues ('dummy' templates) for two model nitro-explosives: TNT (2,4,6-trinitrotoluene) and RDX (Research Department eXplosive, 1,3,5-trinitroperhydro-1,3,5-triazine). This approach afforded a homogenous coverage of gold electrodes with imprinted films of tunable thickness. The electropolymerized molecularly imprinted polydopamine films allowed for a  $10^5$ -fold sensitivity improvement over a bare gold electrode based on tracking the redox peaks of the targets by CV. This improved sensitivity is ascribed to the ability of the MIP to concentrate its target in proximity to the transduction element. The MIP films showed reproducible binding in phosphate buffer (10 mM, pH 7.4), with a dynamic range from 0.1 nM to 10 nM for both TNT and RDX and an increased selectivity over closely related structural analogues.

---

The constantly rising tensions on a world-wide scale and the expanding terroristic threat unfortunately show the need of being able to detect traces of explosives with high sensitivity and selectivity. Despite the wide variety of existing devices, new sensors are yet highly desirable, that provide fast, accurate and continuous monitoring of possibly multiple explosives with just one device. In this perspective, miniaturization and sensors integration into microfluidic systems have become more and more relevant. As an example of a recent trend, microfluidic multisensors coupled to a smartphone readout allow for the simultaneous sensing of several substances, and identification based on pattern recognition.[1–3] The crucial step in developing such devices lies in the development of new selective and sensitive recognition materials, for a straight forward interfacing with a transducer, and an easy manufacturing.

In this context, synthetic biomimetic materials with specific recognition properties such as molecularly imprinted polymers (MIPs) are excellent candidates. MIPs are rigid structures made by co-polymerization of functional and cross-linking monomers in the presence of a molecular template. This templated synthesis allows the functional monomers to self-organize around the template, and the cross-linker to freeze their position into a rigid matrix. Then, the subsequent removal of the template leaves cavities in the MIP, which are complementary to the target in terms of size, shape and distribution of the chemical functionalities. This provides the MIP with high-affinity and high-selectivity binding sites for the template. In specific cases wherein a given target analyte would inhibit polymerization, or would be particularly expensive or of limited availability, structural analogues, also known as “dummies”, can be used to synthesize MIPs.[4,5] Compared to natural systems such as hormone receptors or enzymes, MIPs show a number of advantages, such as compatibility with harsh environments, due to a remarkable temperature and pressure resistance, compatibility with organic media as well as acidic or basic solutions, long storage life and especially low costs.[6,7] MIPs are also easy to interface with transducers, for instance by covalent immobilization of nanoparticles (NPs)[8,9] or by embedding NPs into polymer matrices,[10] or by direct synthesis of thin imprinted films via surface grafting,[11] and electropolymerization,[12] which are particularly advantageous when targeting MIP-based chemosensors.

The use of MIPs for sensing hazardous materials has recently been reviewed by Meng and coworkers,[13] who highlighted the urgent need for devices capable of real-time and on-site detection of explosives and chemical warfare agents. This article puts special emphasis on electrochemical, surface acoustic and optical sensors.[13] Riskin *et al.*[14–16] proposed for example to sense 2,4,6-trinitrotoluene (TNT), RDX (Research Department Explosive, 1,3,5-trinitroperhydro-1,3,5-triazine) and nitroglycerine using MIP films obtained by electropolymerization of bisaniline-modified Au-NPs, for surface plasmon resonance as well as for electrochemical readouts.

Over decades, significant progress has been made in the design of novel electrochemical sensors using different nanocomposites for the sensing of biomolecules, heavy metal ions and pollutants.[17] Recently, electrochemical sensors have been developed for nitrite,[18,19] glucose and H<sub>2</sub>O<sub>2</sub>. [20,21], cadmium ions.[22] Electropolymerization is a powerful tool to generate homogeneous films on electrodes, which can be easily used to reproducibly tune the film thicknesses simply by varying the number of deposition cycles.[23] However, the disadvantage of this technique lies on the limited number of electropolymerizable monomers, which severely reduces the functionalities available for MIP synthesis. In contrast to the widely used free-radical polymerization, MIPs by electropolymerization are formed upon oxidation of a suitable functional monomer in the presence of a template. Dopamine as an electropolymerizable monomer has been reported to interact with different templates by noncovalent interactions such as  $\pi$ - $\pi$  stacking, electrostatic interactions and hydrogen bonding.[24] The first use of dopamine (DA) for molecular imprinting dates back to 2006 by Liu and coworkers,[25] who developed a capacitive sensor for nicotine detection in human serum using molecularly imprinted ultrathin, electropolymerized polydopamine (pDA) films. Recently, Palladino *et al.*[26] reviewed the potential and applications of pDA in (bio)analysis. A wide range of templates was explored spanning from biomolecules (viruses, oligonucleotides, enzymes) to small molecules (sugars, flavorings and phenolic acids). Even though DA shows high potential for the imprinting of many molecules, other electropolymerizable monomers are currently exploited to imprint hazardous materials. For example, a simultaneous chronoamperometric and piezoelectric microgravimetric sensor for nitro-aromatics was proposed by Kutner's group, based on polythiophene(bis(2,2'-bithienyl)-(4-aminophenyl)methane).[27] Mamo *et al.*[28] developed a triacetone triperoxide (TATP) sensor by electropolymerization of pyrrole in presence of TATP for its readout *via* differential pulse voltammetry.

In this work, pDA films targeting either TNT or RDX were imprinted using trimesic acid (TMA)[29] and Kemp's triacid (KA)[15] as structural analogues. The use of dummies came from two main reasons: (i) TNT and RDX are (obviously) commercially available only in small amounts; (ii) the need of performing trace analyses. It is actually well known that the use of a dummy template in MIPs for trace analyses allows to circumvent the problem of template leakage, in case of an incomplete template extraction during the washing step. Thus, structural analogues bearing carboxylic acids rather than nitro groups were chosen as templates, based on volume calculations and literature data.[15,29] Trimesic acid (TMA)[29] and Kemp's triacid (KA)[15] were identified as suitable structural analogues for TNT and RDX, respectively. Moreover, the choice of dopamine as functional monomer was based on computational design using the binding energies for complex formation with both the dummy and the actual target as ranking parameter. The simulations were carried out using DFT (density functional theory) calculations with the  $\omega$ B97X-D/6-31G\* basis set *in silico*. As the best candidate, dopamine offers multiple functional groups for interacting with the template (i.e. hydrogen bonding as well as  $\pi$ - $\pi$  stacking)[24,30] as well as water compatibility.

## MATERIALS AND METHODS

**Materials and Instrumentation.** All chemicals were of analytical grade from either Sigma or VWR and were used as received unless otherwise stated. Explosive standard solutions in acetonitrile were obtained from LGC Standards. For sample and buffer preparation deionized water (18.2 M $\Omega$  cm<sup>-1</sup>) was used. Gold electrodes IDEAU5 were purchased from Metrohm DropSens, Spain.

Molecular modelling calculations with the Spartan 16' software (Wavefunction, Inc.) were carried out on a HP workstation running on Windows 7 Enterprise operating system.

A standard low volume electrochemical cell from Metrohm was used for the measurements and electropolymerization. The gold electrode was used as working electrode, a DRIFREF-2 Ag/AgCl (WPI) was used as reference electrode and a platinum coil as a counter electrode. The measurements were carried out on the Autolab PG stat 12 program. The software used for the recording and post-processing was NOVA 2.0 from Metrohm. The spectra were recorded using cyclic voltammetry in the staircase mode, at a scan rate of 0.02 V s<sup>-1</sup>. The solvent was a 50:1 (v/v) mixture of 10 mM phosphate buffer pH 7.4 and acetonitrile. Acetonitrile was necessary to ensure the TNT solubility.

Scanning electron microscopy (SEM) imaging was carried out on a Quanta FEG 250 scanning electron microscope (Eindhoven, Netherlands). The samples were sputter coated with gold before measurement. Atomic force microscopy (AFM) images were recorded on a Bruker AFM dimension icon and the Gwyddion 2.51 software (Free Open Source software, covered by GNU General Public License) was used to post-process the AFM images.

**Molecular modelling.** The Spartan 2D sketch tool was used to draw the structures of monomers, dummies and targets. They were first minimized with the MMFF94 (Merck Molecular Force Field)[31] force field to obtain an initial geometry and the most stable conformation for each monomer, dummy, target and complex. The lowest-energy conformer was defined as starting geometry in DFT calculations with the  $\omega$ B97X-D/6-31G\* basis set to obtain both the geometry and the thermodynamic parameters of the template-monomer complexes.  $\omega$ B97X-D is a modern density functional capable of accurately predicting both short-range and long-range interactions showing good performance in noncovalently interacting systems.[32,33] Since this approach is time consuming, the calculations for all complexes were carried out with the DFT approach only for monomer, dummy, target molecules and a 1:1 monomer-dummy and 1:1 monomer-target complexes. The suitable functional monomers for the target analytes have been identified based on their binding energy (Figure S1) using the following equation (1):

$$\Delta E_{binding} = E_{complex} - (E_{template} + E_{monomer}) \quad (1)$$

where  $E_{complex}$ ,  $E_{template}$ ,  $E_{monomer}$  are the complex, the template (structural analogue or nitro-explosives) and the monomer energies, respectively.

**Preparation and characterization of MIP and NIP sensors.** The synthesis was performed on gold electrodes according to Weil and coworkers.[34] Briefly, the electrodes were first cleaned with piranha solution (H<sub>2</sub>SO<sub>4</sub>/H<sub>2</sub>O<sub>2</sub> 4:1, v/v) for 20 minutes, then rinsed thoroughly with deionized water and carefully dried with a stream of nitrogen. The electrode was then introduced as working electrode into a low volume electrochemical cell (Metrohm) in a standard three electrode configuration. In a separate vial, a 1 mg mL<sup>-1</sup> dopamine (DA) solution was prepared by dissolving DA·HCl in 10 mM phosphate buffer pH 7.4 while quickly purging with nitrogen. For the molecularly imprinted pDA films, the appropriate amount of template was added depending on the set DA/template ratio (i.e. 20:1, 10:1 or 5:1 molar ratio). Once transferred to the reactor, the solution was further purged with nitrogen before polymerization by CV (4, 8 or 15 cycles) between -0.5 V and +0.5 V, at a scan rate of 0.02 V s<sup>-1</sup>. The electrode was then removed and extensively washed with deionized water, methanol:aqueous ammonia solution at pH 9 (1:1, v/v), methanol and again deionized water before drying with a stream of nitrogen. Each wash lasted for 1 hour under gentle stirring. Reference, non-imprinted pDA films were synthesized as above except that the template was omitted.

The presence of an insulating layer of pDA on top of the gold electrodes was verified using ferro-ferricyanide as a redox probe (5 mM K<sub>4</sub>[Fe(CN)<sub>6</sub>]/K<sub>3</sub>[Fe(CN)<sub>6</sub>] in 10 mM phosphate buffer pH 7.4). The pDA thickness was measured by AFM on half-coated electrodes (e.g. half-immersed in the solution during the electropolymerization). Assuming that pDA would just be present on the immersed part of the IDE, the thickness was estimated as the height-difference between the coated and uncoated parts of the electrode.

**Electrochemical measurements.** Binding studies on MIPs and NIPs (non-imprinted polymers) were performed by immersing the coated electrodes in a solvent mixture based on 50:1 (v/v) 10 mM phosphate buffer pH 7.4/acetonitrile containing the template in concentrations ranging from pM to  $\mu$ M. Cyclic voltammograms were recorded in staircase mode at a scan rate of 0.02 V s<sup>-1</sup> between -0.8 V and 0.8 V for TNT and -1.2 V and 0.8 V for RDX. TNT and RDX concentrations were varied by sequential additions of concentrated stock solution with a syringe. After each injection, the solution was purged with nitrogen for 30 minutes to ensure an oxygen-free atmosphere and a complete equilibrium before measurement.

Selectivity was estimated via displacement tests using a series of structurally related molecules in order to establish to which extent they could replace TNT or RDX. Trimesic acid (TMA), isophthalic acid (IPA) and 4-nitrophenol (4NP) were used as competitors for TNT (50 nM fixed concentration in phosphate buffer pH 7.4 containing increasing amounts of competitor). The replacement by the competitor was calculated as the decrease of the anodic current of TNT at 0.3 V (vs. Ag/AgCl). In a similar way, the selectivity of RDX was tested using structurally related compounds such as KA, glucose (Glu), and TNT while tracking the oxidation peak at +0.4 V (vs. Ag/AgCl).

## RESULTS AND DISCUSSION

*In-silico* screening of optimal functional monomers for MIP films synthesis.

The synthesis of MIPs capable to detect traces of explosives imposes the use of templates which are analogues of the explosives. Therefore, a database with commonly used electropolymerizable monomers for molecular imprinting was first created to screen for the monomer(s) with optimum interaction for both the analogues and the explosives. This database includes dopamine (DA), phenol (P), aminophenylboronate (APB), phenylene diamine (PD), urethane (Ur), furan (Fu), pyrrole (Py), aniline (An) and 3-thiophene acetic acid (TAA). By selecting the functional monomer interacting strongly with the dummy and the target, it is expected to optimize the affinity of the MIP films towards the targeted explosives (TNT and RDX). The calculated binding energies (Table 1) of the 1:1 monomer-dummy and monomer-target complexes in gas phase identified dopamine (Table 1, line 1 highlighted) as the best candidate

for the MIP synthesis towards TMA and KA, the structural analogues of TNT and RDX, respectively (Figure 1). DA shows the lowest

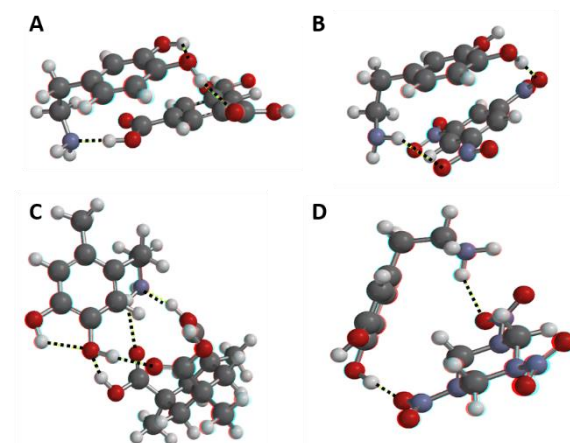


Figure 1: Spartan energy optimized structures in the wB97X-D/6-31G\* basis set (gas phase) for dopamine in complex with TMA (A), TNT (B), KA (C) and RDX (D), respectively. Hydrogen bonds are indicated by dotted lines. CPK coloring was used for the representation of the atoms (white for H, grey for C, blue for N and red for O).

binding energy meaning that it forms the most stable complex individually with the dummies TMA and KA, and also with the target molecules. Our aim was to find out, in addition to the complementarity in size, shape and functionality, the best compromise in terms of strength of interaction that the functional monomer could have together for the dummy and the target, respectively. Both acidic dummies hold carboxylic functional groups capable to act either as a hydrogen bond (H bond) donor via the hydroxyl hydrogen or as a hydrogen bond acceptor via the lone pair electrons of oxygen atoms. Instead, the H bonds formed with the nitro groups[35] are weaker than with the carboxylic acids from the dummies and therefore, the calculated interactions energies with the targets are higher indicating the formation of weaker complexes. The same interaction energy trend was obtained in water calculations using a continuous solvation model.[36]

Table 1. Binding energies (in gas phase) of electropolymerizable functional monomers (FM) for the templates TMA and KA, and for the analytes TNT and RDX.

FM	Binding energy (kcal mol <sup>-1</sup> )			
	TMA	TNT	KA	RDX
DA	<b>-28.21</b>	<b>-16.32</b>	<b>-39.37</b>	<b>-23.39</b>
P	-20.74	-4.69	-29.60	-5.30
APB	-19.71	-11.29	-25.32	-11.90
PD	-17.46	-17.00	-23.95	-8.52
UR	-15.23	-13.65	-21.55	-14.14
Fu	-14.55	-6.00	-23.00	-12.05
Py	-13.30	-15.59	-13.95	-21.65
An	-10.21	-5.33	-18.19	-5.36
TAA	-8.97	-8.89	-14.24	-9.68

Among the minimized structures of the dopamine, dummies and templates, only the lowest energy structure of dopamine is stabilized by one intramolecular OH...O hydrogen bond interaction between the two hydroxyls. In agreement with the literature,[24,30] the optimized structures of the complexes indicate that DA interacts with the dummies and the targets predominantly via hydrogen bond (H<sub>2</sub>N...HO, OH...O=C, HO...HOOC, NH<sub>2</sub>...O<sub>2</sub>N, OH...O<sub>2</sub>N) and  $\pi$ - $\pi$  interactions (Figure 1). These intermolecular acceptor-donor distances vary between 1.8 and 2.2 Å and are therefore characteristic of most predominant hydrogen bonding interaction.[37] In solution, these hydrogen bonds may disrupt but additional hydrogen bonds with the solvent could favor the structure stabilization of the dopamine-functional monomer complex.[38] In addition, a strong cooperativity of individual weak bonds with the template is expected in the growing polymer network during imprinting, and in the final MIP during sensing. The lowest energy structure of the DA complexes has been further analyzed from the perspective of molecular orbitals by calculating the energies of the highest occupied molecular orbital (HOMO) and lowest unoccupied molecular orbital (LUMO).[39] For example, the energy of the LUMO of TMA-DA complex is 7.49 eV higher than the HOMO energy confirming a reasonably stable electronic structure for the complex. LUMO energies varying between 6.34 and 9.47 eV are obtained for the other complexes.

**Electrodeposition of dopamine in the presence or absence of dummy template.** Despite the fact that dopamine can self-polymerize in presence of oxygen at pH higher than 7.4, herein we preferred to apply cyclic voltammetry to drive its polymerization. Indeed, conversely to the spontaneous process, it allows targeting specifically the electrode surface and controlling the film thickness while ensuring a smoother and more homogenous coverage.[23] All these features represent important advantages when designing a sensor. The targets of this study TNT and RDX are both electroactive species, thanks to their nitro-groups which can be reduced to amines. This feature allowed us to specifically track their presence and measure their concentration by cyclic voltammetry (CV). However, electroactivity may represent a downside if it falls in the potential window required by the electropolymerization of the imprinted matrix. Since this is the case with dopamine, the use of a dummy-imprinting approach based on non-electroactive, structural analogues became necessary. Thus, based on volume calculations (Figure S2), we used TMA and KA as dummies for respectively TNT and RDX.

The next step was the synthesis of an imprinted layer on gold electrodes. Figure 2a shows a typical voltammogram for the electropolymerization of dopamine using 15 cycles. During this process, the distinct oxidation and reduction peaks specific for dopamine can be tracked to follow the progressive film growth by monitoring the current decrease cycle after cycle. This is consistent

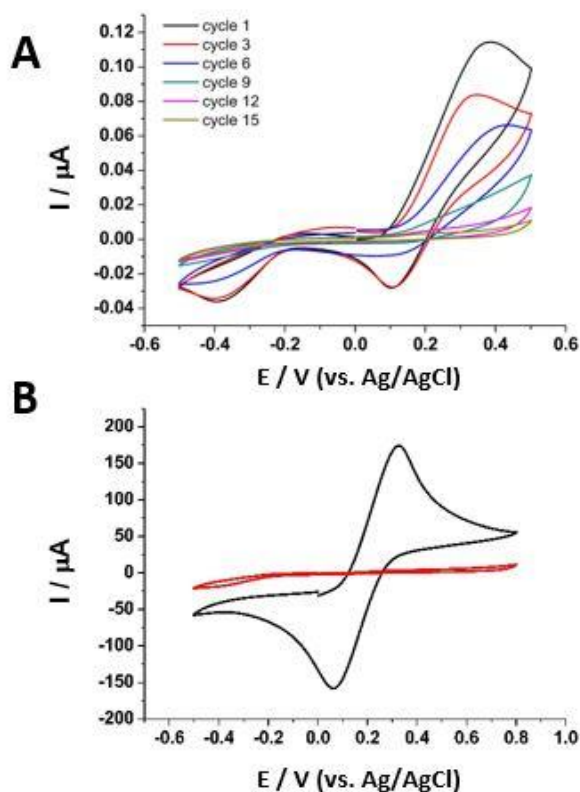
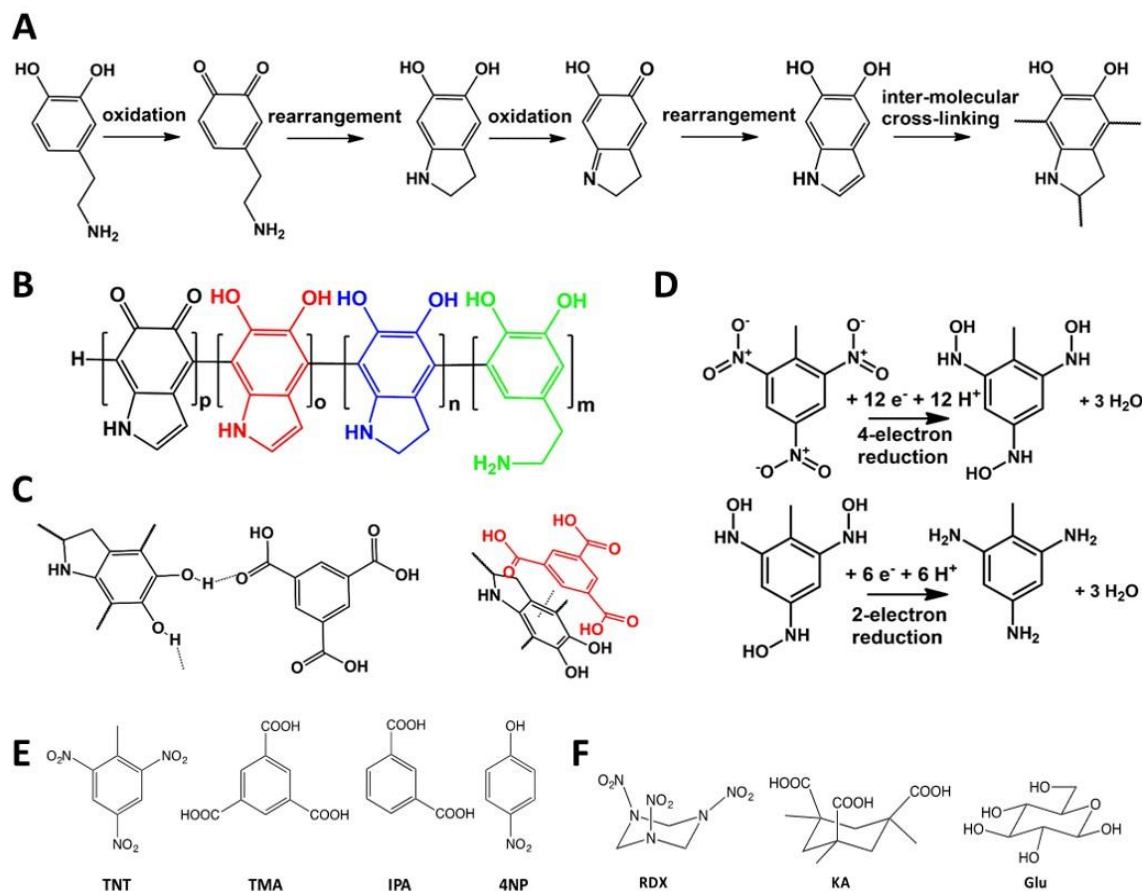


Figure 2: Typical CV profiles for the electropolymerization of a non-imprinted pDA film in phosphate buffer pH 7.4 using up to 15 cycles. A colour code is used to distinguish the CV profiles as function of the number of cycles. (B) Signal blockage of 5 mM ferro/ferricyanide solution upon electropolymerized pDA film on a gold electrode (red) compared with a cyclic voltammogram on a bare electrode (black).

with the insulating character of pDA as previously reported.[25] In the oxidation cycles, the peak at +0.32 V (vs. Ag/AgCl) indicates the formation of dopamine orthoquinone, which subsequently leads to leukodopaminechrome, an aminechrome upon intramolecular cyclization of the dopamine quinone. In the reduction cycles, a peak at +0.09 V (vs. Ag/AgCl) indicates leukodopaminechrome formation. The aminechrome then oxidizes to dopaminedochrome *via* a two-electron transfer, leading to the appearance of a peak for 5,6-dihydroindole at -0.15 V (vs. Ag/AgCl) in the second oxidation cycle. Eventually, it undergoes further polymerization leading to a melanin-like polymer layer. A likely reaction pathway and a probable polymer backbone representation were recently proposed by Ding *et al.*[30] (see Figure 3 A, B).

From the point of view of a selective sensor, achieving a complete coverage of the transduction element is mandatory: indeed, a sensor with only partial coverage on its transducer will suffer from unspecific reading and would then require some surface blocking treatment (e.g. with thiols). To determine the extent of pDA coverage, we measured the signal of a 5 mM ferro/ferricyanide solution in 10 mM phosphate buffer (pH 7.4) used as a redox probe, according to Weil and coworkers.[34] As it can be seen in figure 2B, the massive decrease of the specific oxidation/reduction current of the redox probe (e.g. +0.06 V and +0.32 V vs. Ag/AgCl) suggests that the pDA layer obtained upon 15 CV cycles provided a homogenous and full coverage. A reduction of the number of deposition cycles was also tested (i.e. 4 and 8 cycles), to study the effect on the layer thickness. However, a deposition with only 4 cycles was discarded,



**Figure 3:** Reaction mechanism leading to the polymerization of dopamine pDA (A) and possible backbone structures as proposed by Ding and coworkers (B).[30] Details of potential interactions of pDA with TMA (C). TNT reduction to triamino toluene (D). Structures of the molecules used for the cross selectivity test of TNT (E): 2,4,6-trinitro-toluene (TNT), trimesic acid (TMA), isophthalic acid (IPA) and 4-nitrophenol (4NP), and Research Department eXplosive (RDX) (F): Kemp's triacid (KA) and glucose (Glu).

as the redox probe showed a current intensity similar to that of a bare electrode, thus suggesting an only partial pDA coverage. On the other hand, 8 cycles showed a successful signal blockage consistent with a full coverage.[25] SEM images were also consistent with a full coverage after 8 and 15 cycles, and with an only partial coverage after 4 cycles (Figure S3). One of the advantages of using electropolymerization lies on the possibility of tuning the polymer thickness based on the number of deposition cycles. Thus, we used AFM to probe the pDA thickness on half coated electrodes. By only half-immersing the electrodes in the prepolymerization solution, and by measuring the height difference between the coated and uncoated part of the electrode, we estimated a thickness of 4 and 10 nm respectively after 8 and 15 cycles. Thickness and roughness of our films were both consistent with literature data.[34] In particular, the surface roughness was clearly different before and after polymerization for all the samples. Representative AFM images of a bare and a coated surface can be seen in Figure 4.

Beyond the number of cycles, another important parameter which may affect the polymer coverage and/or thickness could be the ratio between the functional monomer and the template (i.e. DA/template). The ratios that we explored were 20, 10 and 5. Lower ratios were not used to ensure a sufficient rigidity of the MIP network formed. Finally, 15 deposition cycles with a DA:template ratio of 10 yielded the best results, and afforded both NIP and MIP films of 10 nm thickness, together with reproducible sensing results.

The stability of these layers upon washing was also tested. Several conditions were investigated to find a good washing protocol, which finally led to deionized water, methanol:aqueous ammonia, pH 9 (1:1, v/v), methanol and again deionized water, each step for 1h.

After washing, increased anodic and cathodic currents were measured for the redox probe only for the MIP, whereas the NIP showed no detectable changes thus confirming the formation of cavities in the MIP matrix.

**Binding studies.** To test the synthesized MIP films for the binding of their targets, we tracked the specific TNT and RDX peaks related to the reduction of their nitro groups to first hydroxylamines, then to amines (e.g. Figure 3B).[40,41] As it can be seen in Figure 5, the potential sweep generated a current only for the MIP-sensor, whereas the NIP-sensor is completely silent. Measuring the current over a range of concentrations yielded the graphs in Figure 5 (A, C). The imprinted layers yield a typical saturation-type binding isotherm indicating affinity for their targets. Tracking the TNT reduction peak around -0.72 V (vs. Ag/AgCl) (see Figure S4) allowed to measure a dissociation constant ( $K_{app}$ ) of 33 nM (i.e. low affinity binding sites), whereas the oxidation peak at 0.3 V (vs.

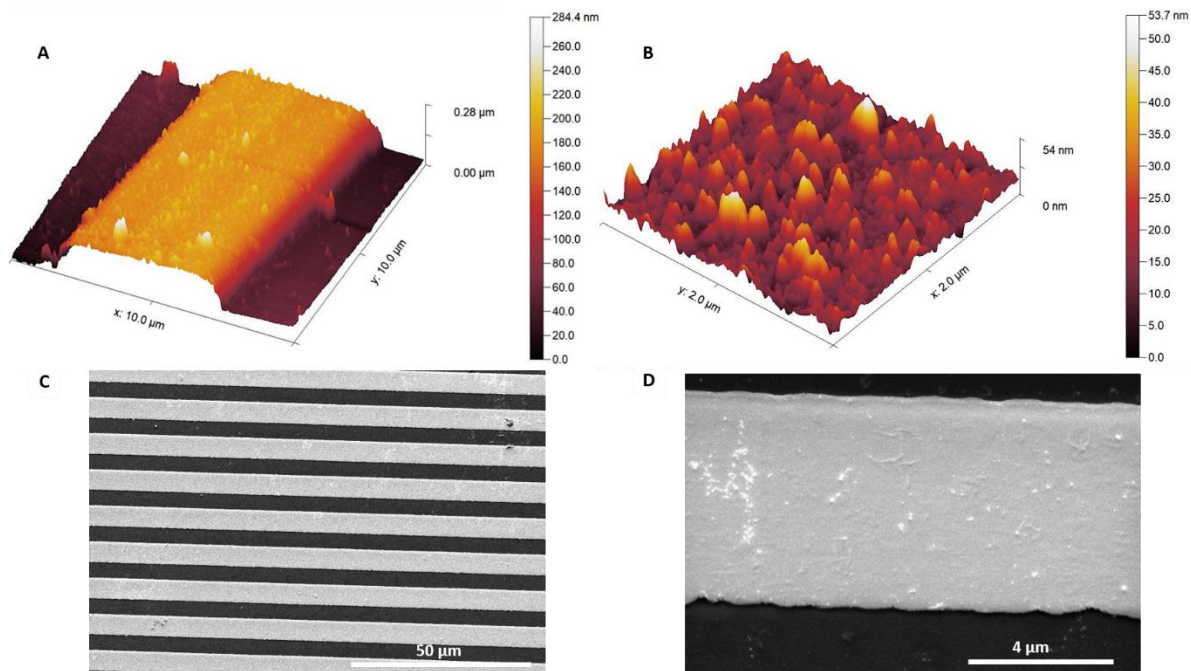


Figure 5: AFM profiles (A, B) and SEM images (C, D) of IDEAU5 coated with p(DA) using 15 cycles. (A) and (C) correspond to the bare electrode whereas (B) and (D) correspond to the imprinted polymer film.

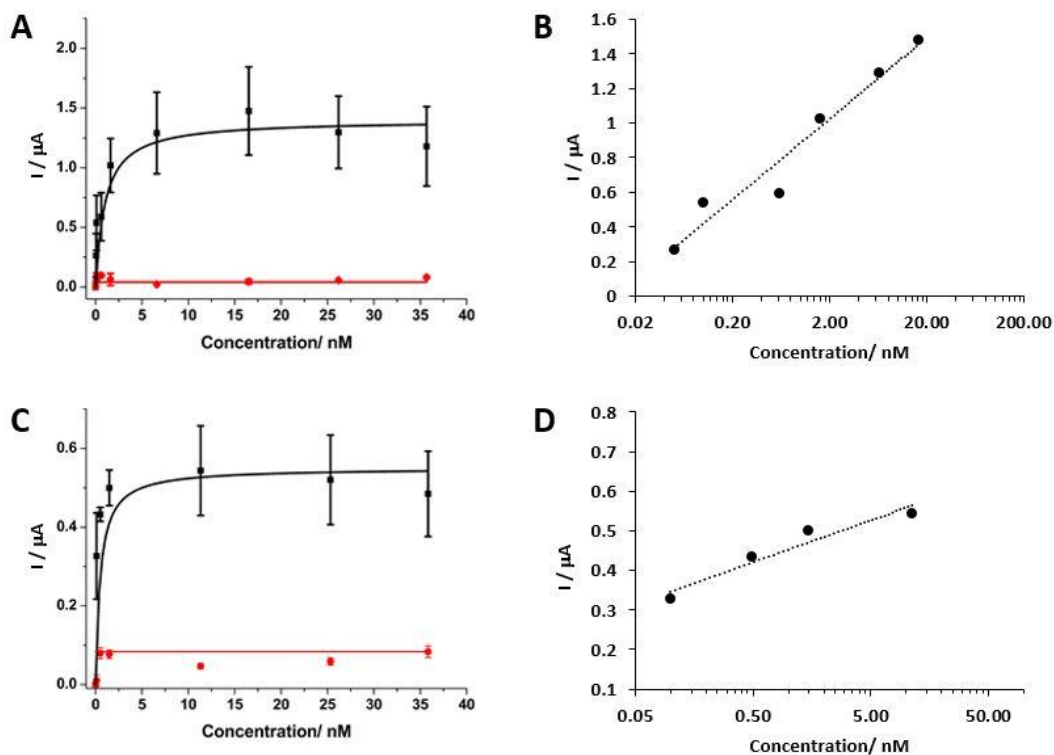


Figure 4: Binding (A,C) and calibration (B, D) curves of TNT (A, B) and RDX (C, D) in phosphate buffer, pH 7.4 by CV obtained as the average of measurements of three different electrodes. (A) TNT binding to the TMA-imprinted (black) and non-imprinted (red) pDA films as a function of TNT concentration at 0.3 V vs. Ag/AgCl. (B) TNT calibration curve on TMA imprinted pDA films and the corresponding trend line ( $y = 0.20\log(x) + 0.88$ ;  $R^2 = 0.95$ ). (C) RDX binding to KA-imprinted (black) and non-imprinted (red) p(DA) films as a function of RDX concentration at 0.4 V vs. Ag/AgCl. (D) RDX calibration curve on KA imprinted pDA films and the corresponding trend line ( $y = 0.05\log(x) + 0.45$ ;  $R^2 = 0.93$ ).

Ag/AgCl) (see Figure 5) appeared to be more suited for low concentrations and allowed to determine a dissociation constant ( $K_{app}$ )

of 0.4 nM (i.e. high affinity binding sites). It will therefore be necessary to switch between these two peaks depending on the sample's concentration. Overall, these results indicate an improved sensitivity over a bare electrode of at least  $10^5$  for both TNT and RDX (Figure S5). Figure 5 (B, D) also shows that both imprinted films for TNT and RDX generate a linear current over a dynamic range from 0.1 nM to 10 nM, which makes them suitable for quantification. More specifically, we measured a linear range for TNT between 50 pM and 16 nM, whereas that of RDX spanned from 100 pM to 11 nM

The limit of detection (LOD) for TNT was 50 pM, while that of RDX was 100 pM. On the other hand, sensitivity was obtained as 0.20  $\mu\text{A}/\log(\text{pM})$  for TNT and 0.05  $\mu\text{A}/\log(\text{pM})$  for RDX. Once the binding properties for TNT were characterized, selectivity studies were conducted using a series of structurally related yet electro-inactive molecules (in the used potential window), in order to establish to which extent they could replace TNT in the binding sites. Thus, increasing concentrations of respectively TMA, IPA and 4NP (Table 2) were incubated with a fixed concentration of TNT and the decrease of TNT peak current was used to establish the degree of displacement by the competitor. TMA is the dummy template used for the imprinting, while IPA and 4NP are both smaller than TNT and can therefore access the binding sites. The data in Table 2 were obtained by tracking the anodic current of TNT at 0.3 V (vs. Ag/AgCl) incubated with an increasing amount of competitors and calculated as percentage of the target still bound. These tests performed with 50 nM TNT solutions in phosphate buffer pH 7.4 showed that TMA-imprinted pDA binds TNT very well, more strongly than the template TMA, since more than a tenfold excess is needed for partially displacing TNT. Interestingly, IPA also showed some affinity, whereas 4NP provided the lowest effect. Thus, TMA-imprinted pDA are really selective for TNT.

Films imprinted with Kemp's triacid for RDX sensing were also synthesized and characterized following the same rationale. The results obtained upon tracking the binding *via* the oxidation peak at 0.4 V (vs. Ag/AgCl) showed that the MIP can detect the presence of RDX down to the pM range, with a dissociation constant of 0.06 nM, while the NIP is once again virtually insensitive to it (Figure 5C). For higher concentrations, the cathodic current measured at  $-1.04$  V (vs. Ag/AgCl) showed to be more effective, as already noticed for TNT.

We also tested the RDX selectivity by displacement tests (Table 2) using structurally related compounds, such as Kemp's acid and glucose. In the case of glucose, the higher affinity compared to TMA may be due to its smaller size and to its equilibrium between open and closed structure, which operates in water at any pH and allows it to easily fit into the binding sites. Interestingly, when using KA-imprinted pDA to bind TNT (Figure S6), a much higher dissociation constant was obtained (i.e. 3.5 nM vs. 0.06 nM), indicating that KA is a poor template dummy for TNT, conversely to TMA. This also justifies the rational choice of the target analogues as templates for the different explosives. In the perspective of using these MIP sensors for measuring either TNT or RDX concentration, their binding data were converted into a semi logarithmic scale (Figure 5C, D), which resulted in linear calibration curves able to cover a concentration range extending for more than two orders of magnitude.

**Table 2. Competitive measurements of TNT and RDX incubated with increasing amounts of competitors.**

# molar equivalent	Bound TNT (%)			Bound RDX (%)	
	TMA	IPA	4NP	KA	Glu
0	100	100	100	100	100
1	98.2 $\pm$ 0.6	98.5 $\pm$ 0.9	99.3 $\pm$ 0.6	99.3 $\pm$ 0.9	95.6 $\pm$ 0.6
2	97.3 $\pm$ 1.0	77.3 $\pm$ 1.5	94.9 $\pm$ 1.0	98.2 $\pm$ 1.9	85.4 $\pm$ 1.1
10	94.1 $\pm$ 0.9	74.2 $\pm$ 1.3	93.6 $\pm$ 1.6	96.9 $\pm$ 2.1	84.9 $\pm$ 0.9
20	43.0 $\pm$ 2.0	46.1 $\pm$ 3.4	86.0 $\pm$ 2.6	91.4 $\pm$ 3.4	68 $\pm$ 2.6

## CONCLUSIONS

In this paper a rational approach for sensing TNT and RDX using electropolymerized imprinted polydopamine films is proposed, as well as the optimization and characterization of such prepared films. This approach is well suited especially for lab-on-a-chip designs and sensor arrays as the polymer deposition can be locally confined on a targeted electrode in the case of a chip. Our strategy relies on *in silico* screening of an electropolymerizable functional monomer capable to find the best candidate displaying high affinity for both the dummy molecule and the actual target. Hence, based density functional theory calculations with the  $\omega\text{B97X-D}/6\text{-31G}^*$  basis set, dopamine was identified as the best functional monomer and its electropolymerization with trimesic acid or Kemp's acid as dummy templates for respectively TNT and RDX was easily achieved by cyclic voltammetry. The homogeneous films thus obtained show high affinity for their targets, conversely to non-imprinted reference films. Also, these films allowed sensing TNT and RDX in the pM range, which is at least five orders of magnitude lower than the sensitivity reached on a bare electrode.

Interestingly, these films also displayed selectivity over structurally related analogues, as demonstrated by testing the binding of TNT in the presence of structural analogues such as trimesic acid, isophthalic acid, 4-nitrophenol, and the binding of RDX in the presence of Kemp's acid and glucose. Additionally, TNT binding to a KA-imprinted pDA film was studied, showing again less affinity than the target RDX.

The cyclic voltammetry approach presented here allows to simultaneously monitor and discriminate the different nitro-explosives *via* their specific redox peaks, which is an additional advantage in the perspective of analyzing an unknown sample. Overall, these results confirm the high potential of dopamine also as an electropolymerizable monomer for MIP films on electrodes, for sensing hazardous materials.

## ASSOCIATED CONTENT

**Supporting Information.** *In-silico* screening of the best monomer for both explosive and analogue. Calculated volume for TNT and RDX explosives and their structural analogues. Voltammograms (4 cycles pDA deposition), SEM and AFM images. Binding of TNT binding by CV over TMA-imprinted pDA. CV profiles for TNT solution on a bare electrode and pDA MIP film. Binding of TNT binding by CV over KA-imprinted pDA. This material is available free of charge via the Internet at <http://pubs.acs.org>.

## AUTHOR INFORMATION

### Corresponding Author

\* [carlo.gonzato@utc.fr](mailto:carlo.gonzato@utc.fr); [karsten.haupt@utc.fr](mailto:karsten.haupt@utc.fr)

### Present Address

‡ Université du Sud Toulon, Laboratoire Matériaux Polymères-Interfaces-Environnement Marin, 83957 La Garde Cedex, France.

### Author Contributions

K.H conceived the idea. N.L. synthesized the polydopamine films and performed the CV experiments. L.D. performed and analyzed the DFT calculations. K. H., L.D. and C.G. directed the work. N.L., L.D. C.G. and K.H. analyzed the results and wrote the manuscript. All authors reviewed and approved the manuscript.

### Funding Sources

This work was financially supported by the European Commission (project NOSY for New Operational Sensing sYstems, Grant agreement ID 653839, H2020-EU.3.7).

### Declaration of Competing Interest

The authors declare no competing financial interests or personal relationships that could have appeared to influence the work reported in this paper.

## ACKNOWLEDGMENT

We thank Frederic Nadaud from the Physicochemical Analysis Group at the Compiègne University of Technology for AFM and SEM images. We are also grateful to Jeremy Terrien from the Electronic Service at the Compiègne University of Technology for help with the electrochemical installation. NL also thanks Lea Ledaine and Ioanna Tereza Gad for their experimental support during their internships.

## ABBREVIATIONS

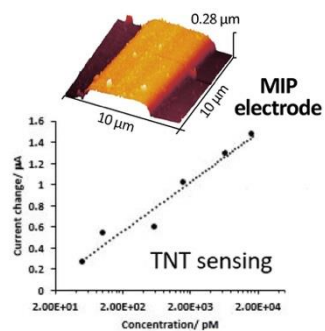
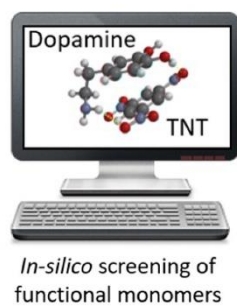
ACN acetonitrile; AFM atomic force microscopy; APB aminophenylboronate; An aniline; CV cyclic voltammetry; DA dopamine; DFT density functional theory; Fu furan; Glu glucose; IDE interdigitated electrode; IPA isophthalic acid; KA Kemp's triacid; MIP molecularly imprinted polymer; MMFF94 Merck Molecular Force Field 94; 4NP 4-nitrophenol; NIP non imprinted polymer; NPs nanoparticles; P phenol; PBS phosphate buffer; PD phenylene diamine; p(DA) polydopamine; Py pyrrole; RDX Re-search Department eXplosive, 1,3,5-trinitroperhydro-1,3,5-triazine; SEM scanning electron microscopy; TAA 3-thiophene acetic acid; TATP triacetone triperoxide; TMA trimesic acid; TNT 2,4,6-trinitrotoluene; Ur urethane (ethyl carbamate).

## REFERENCES

- [1] W. Xiao, M. Xiao, Q. Fu, S. Yu, H. Shen, H. Bian, Y. Tang, A portable smart-phone readout device for the detection of mercury contamination based on an aptamer-assay nanosensor, *Sensors*. 16 (2016) 1871. <https://doi.org/10.3390/s16111871>.
- [2] W. Lu, X. Dong, L. Qiu, Z. Yan, Z. Meng, M. Xue, X. He, X. Liu, Colorimetric sensor arrays based on pattern recognition for the detection of nitroaromatic molecules, *J. Hazard. Mater.* 326 (2016) 130–137. <https://doi.org/10.1016/j.jhazmat.2016.12.024>.
- [3] S. Majumder, M.J. Deen, Smartphone sensors for health monitoring and diagnosis, *Sensors*. 19 (2019) 1–45. <https://doi.org/10.3390/s19092164>.
- [4] G. Wulff, Molecular imprinting in cross-linked materials with the aid of molecular templates — A way towards artificial antibodies, *Angew. Chem. Int. Ed.* 34 (1995) 1812–1832. <https://doi.org/10.1002/anie.199518121>.
- [5] K. Haupt, Imprinted polymers — Tailor-made mimics of antibodies and receptors, *Chem. Commun.* (2003) 171–178.
- [6] J. Svenson, I.A. Nicholls, On the thermal and chemical stability of molecularly imprinted polymers, *Anal. Chim. Acta.* 435 (2001) 19–24. [https://doi.org/10.1016/S0003-2670\(00\)01396-9](https://doi.org/10.1016/S0003-2670(00)01396-9).
- [7] K. Smolinska-Kempisty, A. Guerreiro, F. Canfarotta, C. Cáceres, M.J. Whitcombe, S. Piletsky, A comparison of the performance of molecularly imprinted polymer nanoparticles for small molecule targets and antibodies in the ELISA format, *Sci. Rep.* 6 (2016) 1–7. <https://doi.org/10.1038/srep37638>.
- [8] T. Kamra, S. Chaudhary, C. Xu, N. Johansson, L. Montelius, J. Schnadt, L. Ye, Covalent immobilization of molecularly imprinted polymer nanoparticles using an epoxy silane, *J. Colloid Interface Sci.* 445 (2015) 277–284. <https://doi.org/10.1016/j.jcis.2014.12.086>.
- [9] T. Kamra, S. Chaudhary, C. Xu, L. Montelius, J. Schnadt, L. Ye, Covalent immobilization of molecularly imprinted polymer nanoparticles on a gold surface using carbodiimide coupling for chemical sensing, *J. Colloid Interface Sci.* 461 (2016) 1–8. <https://doi.org/10.1016/j.jcis.2015.09.009>.
- [10] K. Prasad, K.P. Prathish, J.M. Gladis, G.R.K. Naidu, T.P. Rao, Molecularly imprinted polymer (biomimetic) based potentiometric sensor for atrazine, *Sensors Actuators, B Chem.* 123 (2007) 65–70. <https://doi.org/10.1016/j.snb.2006.07.022>.
- [11] A. Bossi, M.J. Whitcombe, Y. Uludag, S. Fowler, I. Chianella, S. Subrahmanyam, I. Sanchez, S.A. Piletsky, Synthesis of controlled polymeric cross-linked coatings via iniferter polymerisation in the presence of tetraethyl thiuram disulphide chain terminator, *Biosens. Bioelectron.* 25 (2010) 2149–2155. <https://doi.org/10.1016/j.bios.2010.02.015>.

- [12] P.S. Sharma, A. Pietrzyk-Le, F. D'Souza, W. Kutner, Electrochemically synthesized polymers in molecular imprinting for chemical sensing, *Anal. Bioanal. Chem.* 402 (2012) 3177–3204. <https://doi.org/10.1007/s00216-011-5696-6>.
- [13] W. Lu, M. Xue, Z. Xu, X. Dong, F. Xue, F. Wang, Q. Wang, Z. Meng, Molecularly imprinted polymers for the sensing of explosives and chemical warfare agents, *Curr. Org. Chem.* 19 (2015) 62–71. <https://doi.org/10.2174/1385272819666141201215551>.
- [14] M. Riskin, R. Tel-Vered, T. Bourenko, E. Granot, I. Willner, Imprinting of molecular recognition sites through electropolymerization of functionalized Au nanoparticles: Development of an electrochemical TNT sensor based on  $\pi$ -donor-acceptor interactions, *J. Am. Chem. Soc.* 130 (2008) 9726–9733. <https://doi.org/10.1021/ja711278c>.
- [15] M. Riskin, R. Tel-Vered, I. Willner, Imprinted Au-nanoparticle composites for the ultrasensitive surface plasmon resonance detection of hexahydro-1,3,5-trinitro-1,3,5-triazine (RDX), *Adv. Mater.* 22 (2010) 1387–1391. <https://doi.org/10.1002/adma.200903007>.
- [16] M. Riskin, Y. Ben-Amram, R. Tel-Vered, V. Chegel, J. Almog, I. Willner, Molecularly imprinted Au nanoparticles composites on Au surfaces for the surface plasmon resonance detection of pentaerythritol tetranitrate, nitroglycerin, and ethylene glycol dinitrate, *Anal. Chem.* 83 (2011) 3082–3088. <https://doi.org/10.1021/ac1033424>.
- [17] R. Ramachandran, T.-W. Chen, S.-M. Chen, T. Baskar, R. Kannan, P. Elumalai, P. Raja, T. Jeyapragasam, K. Dinakaran, G.P. Gnana Kumar, A review of the advanced developments of electrochemical sensors for the detection of toxic and bioactive molecules, *Inorg. Chem. Front.* 6 (2019) 3418–3439.
- [18] R. Cao, H. Huang, J. Liang, T. Wang, Y. Luo, A.M. Asiri, H. Ye, X. Sun, A MoN nanosheet array supported on carbon cloth as an efficient electrochemical sensor for nitrite detection, *Analyst.* 144 (2019) 5378–5380. <https://doi.org/10.1039/c9an01270b>.
- [19] R. Wang, Z. Wang, X. Xiang, R. Zhang, X. Shi, X. Sun, MnO<sub>2</sub> nanoarrays: an efficient catalyst electrode for nitrite electroreduction toward sensing and NH<sub>3</sub> synthesis applications, *Chem. Commun.* 54 (2018) 10340–10342. <https://doi.org/10.1039/c8cc05837g>.
- [20] F. Xie, X. Cao, F. Qu, A.M. Asiri, X. Sun, Cobalt nitride nanowire array as an efficient electrochemical sensor for glucose and H<sub>2</sub>O<sub>2</sub> detection, *Sensors Actuators, B Chem.* 255 (2018) 1254–1261. <https://doi.org/10.1016/j.snb.2017.08.098>.
- [21] Z. Wang, X. Cao, D. Liu, S. Hao, R. Kong, G. Du, A.M. Asiri, X. Sun, Copper-Nitride Nanowires Array: An Efficient Dual-Functional Catalyst Electrode for Sensitive and Selective Non-Enzymatic Glucose and Hydrogen Peroxide Sensing, *Chem. - A Eur. J.* 23 (2017) 4986–4989. <https://doi.org/10.1002/chem.201700366>.
- [22] Y. Si, J. Liu, Y. Chen, X. Miao, F. Ye, Z. Liu, J. Li, rGO/AuNPs/tetraphenylporphyrin nanoconjugate-based electrochemical sensor for highly sensitive detection of cadmium ions, *Anal. Methods.* 10 (2018) 3631–3636. <https://doi.org/10.1039/c8ay01020j>.
- [23] B. Stöckle, D.Y.W. Ng, C. Meier, T. Paust, F. Bischoff, T. Diemant, R.J. Behm, K.E. Gottschalk, U. Ziener, T. Weil, Precise control of polydopamine film formation by electropolymerization, *Macromol. Symp.* 346 (2014) 73–81. <https://doi.org/10.1002/masy.201400130>.
- [24] D.R. Dreyer, D.J. Miller, B.D. Freeman, D.R. Paul, C.W. Bielawski, Perspectives on poly(dopamine), *Chem. Sci.* 4 (2013) 3796–3802. <https://doi.org/10.1039/c3sc51501j>.
- [25] K. Liu, W.Z. Wei, J.X. Zeng, X.Y. Liu, Y.P. Gao, Application of a novel electrosynthesized polydopamine-imprinted film to the capacitive sensing of nicotine, *Anal. Bioanal. Chem.* 385 (2006) 724–729. <https://doi.org/10.1007/s00216-006-0489-z>.
- [26] P. Palladino, F. Bettazzi, S. Scarano, Polydopamine: surface coating, molecular imprinting, and electrochemistry—successful applications and future perspectives in (bio)analysis, *Anal. Bioanal. Chem.* 411 (2019) 4327–4338. <https://doi.org/10.1007/s00216-019-01665-w>.
- [27] T.-P. Huynh, M. Sosnowska, J.W. Sobczak, C.B. KC, V.N. Nesterov, F. D'Souza, W. Kutner, Simultaneous chronoamperometry and piezoelectric microgravimetry determination of nitroaromatic explosives using molecularly imprinted thiophene polymers, *Anal. Chem.* 85 (2013) 8361–8368. <https://doi.org/10.1021/ac4017677>.
- [28] S.K. Mamo, J. Gonzalez-Rodriguez, Development of a molecularly imprinted polymer-based sensor for the electrochemical determination of triacetone triperoxide (TATP), *Sensors.* 14 (2014) 23269–23282. <https://doi.org/10.3390/s141223269>.
- [29] B. Sellergren, A.J. Hall, Method for producing molecularly imprinted polymers for the recognition of target molecules, *US20080038832A1*, 2008.
- [30] Y.H. Ding, M. Floren, W. Tan, Mussel-inspired polydopamine for bio-surface functionalization, *Biosurface and Biotechnology.* 2 (2016) 121–136. <https://doi.org/10.1016/j.bsbt.2016.11.001>.
- [31] T.A. Halgren, Molecular geometries and vibrational frequencies for MMFF94, *J. Comput. Chem.* 17 (1996) 553–586.
- [32] Y. Minenkov, Å. Singstad, G. Occhipinti, V.R. Jensen, The accuracy of DFT-optimized geometries of functional transition metal compounds: A validation study of catalysts for olefin metathesis and other reactions in the homogeneous phase, *Dalt. Trans.* 41 (2012) 5526–5541. <https://doi.org/10.1039/c2dt12232d>.
- [33] B.R. Brooks, C.L.B. III, J. A. D. Mackerell, L. Nilsson, R.J. Petrella, B. Roux, Y. Won, G. Archontis, C. Bartels, S. Boresch, A. Caffisch, L. Caves, Q. Cui, A.R. Dinner, M. Feig, S. Fischer, J. Gao, M.W.I. Hodoscsek, M. Karplus, Semiempirical GGA-type density functional constructed with a long-range dispersion correction, *J. Comput. Chem.* 30 (2009) 1545–1614. <https://doi.org/10.1002/jcc>.
- [34] B. Stöckle, D.Y.W. Ng, C. Meier, T. Paust, F. Bischoff, T. Diemant, R.J. Behm, K.E. Gottschalk, U. Ziener, T. Weil, Precise control of polydopamine film formation by electropolymerization, *Macromol. Symp.* 346 (2014) 73–81. <https://doi.org/10.1002/masy.201400130>.
- [35] W.F. Baitinger, P. von R. Schleyer, T.S.S.R. Murty, L. Robinson, Nitro groups as proton acceptors in hydrogen bonding, *Tetrahedron.* 20 (1964) 1635–1647. [https://doi.org/10.1016/S0040-4020\(01\)99161-6](https://doi.org/10.1016/S0040-4020(01)99161-6).
- [36] A. V. Marenich, R.M. Olson, C.P. Kelly, C.J. Cramer, D.G. Truhlar, Self-consistent reaction field model for aqueous and nonaqueous solutions based on accurate polarized partial charges, *J. Chem. Theory Comput.* 3 (2007) 2011–2033. <https://doi.org/10.1021/ct7001418>.
- [37] Sławomir Grabowski, *Hydrogen Bonding - New Insights*, Springer, 2006.
- [38] P.I. Nagy, Competing intramolecular vs. Intermolecular hydrogen bonds in solution, *Int. J. Mol. Sci.* 15 (2014) 19562–19633. <https://doi.org/10.3390/ijms151119562>.
- [39] T. Sajini, S. John, B. Mathew, Rational design and tailoring of imprinted polymeric enantioselective sensor layered on multiwalled carbon nanotubes for the chiral recognition of d -mandelic acid , *Polym. Chem.* 10 (2019) 5364–5384. <https://doi.org/10.1039/c9py01003c>.
- [40] J.S. Caygill, S.D. Collyer, J.L. Holmes, F. Davis, S.P.J. Higson, Disposable screen-printed sensors for the electrochemical detection of TNT and DNT, *Analyst.* 138 (2013) 346–352. <https://doi.org/10.1039/c2an36351h>.
- [41] A. Üzer, Ş. Sağlam, Y. Tekdemir, B. Ustamehmetoğlu, E. Sezer, E. Erçağ, R. Apak, Determination of nitroaromatic and nitramine type energetic materials in synthetic and real mixtures by cyclic voltammetry, *Talanta.* 115 (2013) 768–778. <https://doi.org/10.1016/j.talanta.2013.06.047>.

## Table of Contents artwork



### Highlights:

- CV sensors for nitro-explosives
- polydopamine-imprinted films
- molecular modelling